Angiogenesis (2019) 22:211–221
https://doi.org/10.1007/s10456-019-09663-3

BRIEF COMMUNICATION

A ribosomal DNA-hosted microRNA regulates zebrafish embryonic angiogenesis

Yunwei Shi[1] · Xuchu Duan[2] · Guangmin Xu[1] · Xiaoning Wang[1] · Guanyun Wei[2] · Shikui Dong[3] · Gangcai Xie[1,4] · Dong Liu[1]

Received: 31 July 2018 / Accepted: 8 January 2019 / Published online: 17 January 2019

Abstract

MicroRNAs (miRNAs) are single-stranded small non-coding RNAs, generally 18–25 nucleotides in length, that act as repressors of gene expression. miRNAs are encoded by independent genes or processed from a variety of different RNA species. So far, there is no evidence showing that the ribosomal DNA-hosted microRNA is implicated in vertebrate development. Currently, we found a highly expressed small RNA hosted in ribosomal DNA was predicted as a novel miRNA, named miR-ntu1, in zebrafish endothelial cells by deep sequencing analysis. The miRNA was validated by custom-designed Taqman PCR, Northern Blot, and in silico analysis. Furthermore, we demonstrated that miR-ntu1 played a crucial role in zebrafish angiogenesis via modulation of Notch signaling. Our findings provide a notable case that a miRNA hosted in ribosomal DNA is involved in vertebrate development.

Keywords MiRNA · Ribosomal DNA · Endothelial cells · Zebrafish · Angiogenesis

Introduction

MicroRNAs (miRNAs) are single-stranded small non-coding RNAs, generally 18–25 nucleotides in length, that act as repressors of gene expression [1–3]. MiRNAs can be encoded by independent genes which contain their own miRNA gene promoter and regulatory units, but also can be processed from a variety of different RNA species, including introns, exons, 3′ UTRs of mRNAs, long non-coding RNAs, snoRNAs, and transposons [1, 4, 5]. MiRNAs have been involved in diverse roles in fundamental biological processes and various aspects of animal development [6, 7], including cardiovascular development and disease [8–11].

The eukaryotic ribosome contains four Ribosomal RNAs (rRNA), including 5S, 5.8S, 18S, and 28S rRNAs, which are essential for the structure and function of ribosomes, and transcribed by RNA polymerase [12]. Lately, Chak et al. reported a non-canonical miRNA hosted by ribosomal DNA in Drosophila [13]. So far, there is no evidence showing that the ribosomal DNA-hosted microRNA is implicated in vertebrate development. Here we show that a ribosomal DNA-hosted microRNA expressed in endothelial cells (ECs) regulates zebrafish embryonic blood vessel formation.

Yunwei Shi, Xuchu Duan, and Guangmin Xu contributed equally to this work.

Electronic supplementary material The online version of this article (https://doi.org/10.1007/s10456-019-09663-3) contains supplementary material, which is available to authorized users.

✉ Gangcai Xie
gangcai@ntu.edu.cn

✉ Dong Liu
liudongtom@gmail.com; tom@ntu.edu.cn

[1] Co-innovation Center of Neuroregeneration, Key Laboratory of Neuroregeneration of Jiangsu and Ministry of Education, Nantong University, Qixiu Road 19, Nantong 226001, China

[2] School of Life Science, Nantong University, Nantong, China

[3] Department of Sports Medicine, Shanghai Jiao Tong University Affiliated Sixth People's Hospital, Shanghai, China

[4] Medical School, Institute of Reproductive Medicine, Nantong University, Qixiu Road 19, Nantong 226001, China

Results

Identification of a novel miRNA miR-ntu1 in zebrafish endothelial cells

To characterize the expression profile of miRNAs in ECs of developing zebrafish blood vessels, we isolated the GFP + cells in *Tg(kdrl:EGFP)* zebrafish embryos at 22 h post-fertilization (hpf) by fluorescence-activated cell sorting (FACS). The purity of these GFP + cells was validated by FAC resorting analysis and Taqman PCR analysis of marker genes of the ECs as we previously did [14]. Endothelial miRNA expression profiles were obtained by deep sequencing analysis. The known and novel miRNAs were identified by miRDeep2 [15, 16]. The experimental pipeline was delineated in diagram (Fig. 1a). Interestingly, we found that a highly expressed small RNA, 20 nucleotides in length, was predicted as a novel miRNA, whose precursor sequence could form a stem-loop structure (Fig. 1b, c). There are 109,806 reads mapped to the predicted miRNA hairpin and are contained in the sequence covered by the predicted mature miRNA (Fig. 1b, Supplementary Data 1). In addition, 79 reads were mapped to the predicted miRNA hairpin and are contained in the sequence covered by the predicted star miRNA (Fig. 1b, Supplementary Data 1). The mature sequence of this predicted miRNA was validated by northern blot (Fig. 2a). Since it has not been registered in miRBase Release 21, we named it miR-ntu1. The expression level of miR-ntu1 is higher than those of the endothelial specific miR-126s, miR-30s, and miR-10s, while it is lower than the expression of miR-144 (Fig. 1d). Through blat analysis of miR-ntu1 in zebrafish genome, it was mapped to 4 RepeatMasker loci in the zebrafish GRCz10/danRer10, all named LSU-rRNA_Hsa of rRNA family (Supplementary Fig. 1).

miR-ntu1 regulates angiogenesis during development

Since miR-ntu1 is highly expressed in zebrafish embryonic ECs, we reasoned that it might modulate the blood vessel formation. For determining whether this was the case, we designed antisense oligonucleotide morpholinos

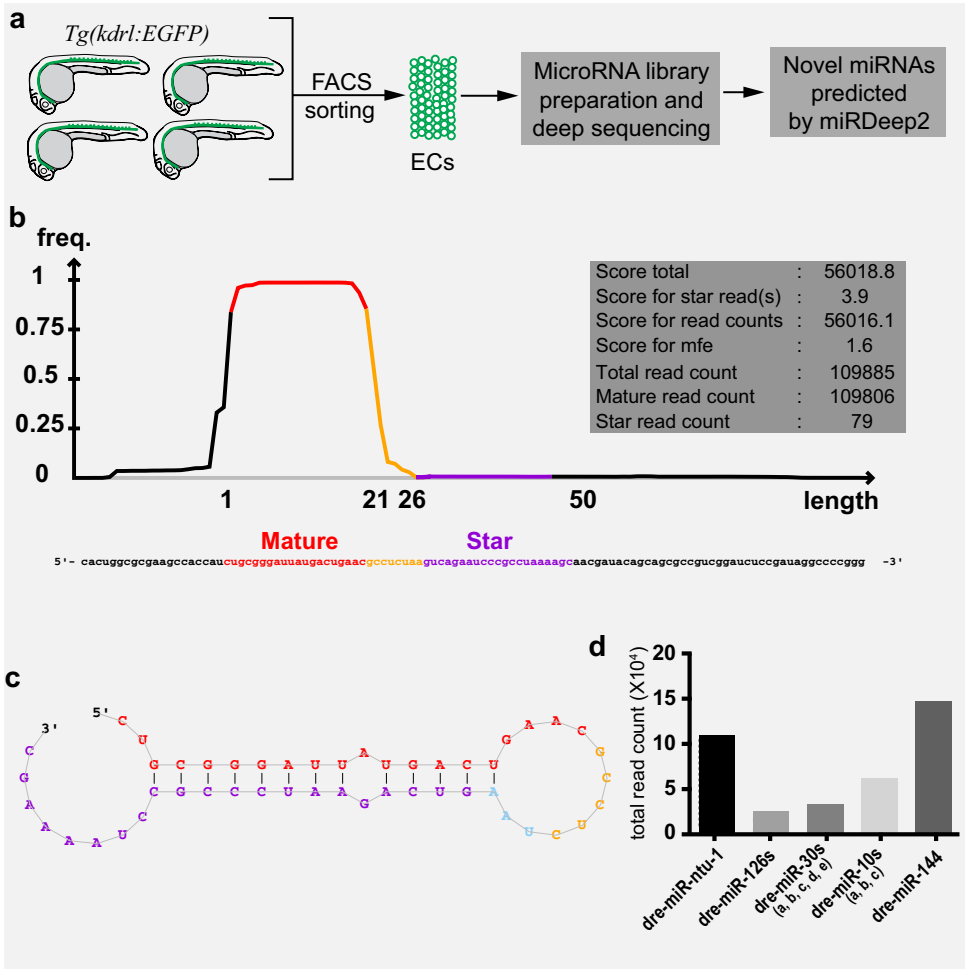

Fig. 1 Identification of miR-ntu1. **a** The experimental pipeline of identification of miR-ntu1 in zebrafish ECs. **b** The read frequency of mature and star miR-ntu1. **c** The predicated structure of pri-miR-ntu1. **d** The relative expression of miR-ntu1 compared with miR-144, miR-10s, and miR-126s, which are specifically expressed in ECs

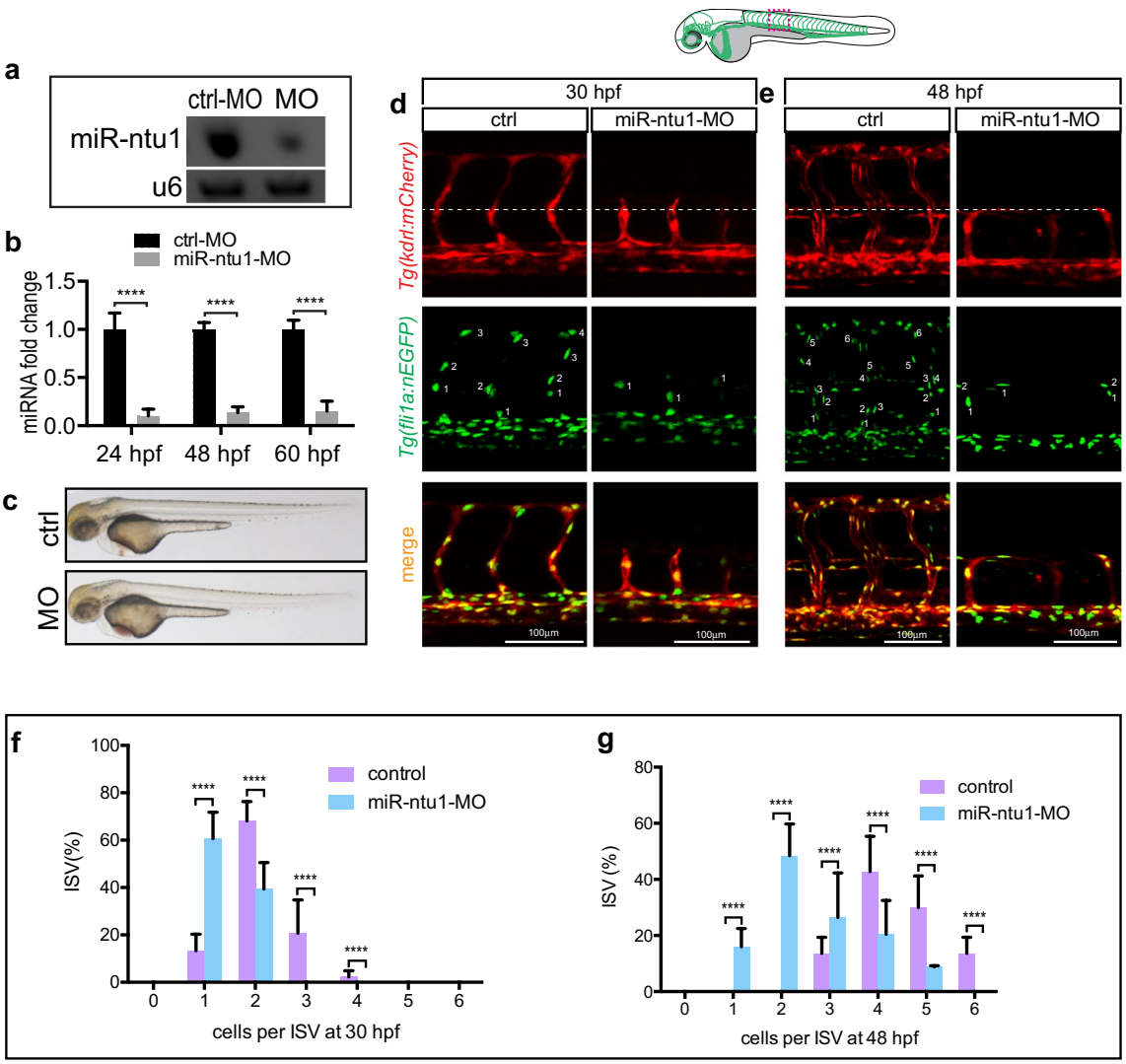

Fig. 2 miR-ntu1 loss of function results in the blood vessel morphogenesis defects in zebrafish embryos. **a** Northern blot analysis for miR-ntu1 in control and miR-ntu1-MO-injected embryos. **b** Quantitative PCR analysis of control and miR-ntu1-MO-injected embryos using the custom-designed TaqMan probe (experiments repeated 3 times; independent samples = 6). *T* test; ****$P < 0.0001$. **c** Zebrafish embryos of control and miR-ntu1 morphants at 48 hpf imaged in bright field. **d, e** Confocal imaging analysis of blood vessel in control and miR-ntu1-MO-injected *Tg(kdrl:mCherry::fli1a:nEGFP)* embryos at 30 hpf and 48 hpf. The white dash lines indicate the position of horizontal myoseptum. **f, g** Percent of ISVs with indicated cells/ISV in control or miR-ntu1-MO-injected embryos at 30 hpf (experiments repeated 3 times; control, $n = 18$; miR-ntu1-MO, $n = 25$) and 48 hpf (experiments repeated 3 times; control, $n = 20$; miR-ntu1-MO, $n = 21$). *T* test; ****$P < 0.0001$

for blocking miR-ntu1. A guide-dicer targeted oligo (miR-ntu1-MO) was validated to efficiently reduced levels of mature miR-ntu1 using Northern Blot and miRNA custom-designed Taqman PCR (Fig. 2a, b). The miR-ntu1 morphant zebrafish embryos grossly look normal (Fig. 2c; Supplementary Fig. 2a). However, the blood vessel outgrowth is severely disrupted. In control embryo, the intersegmental vessels (ISV) sprout from the dorsal aorta (DA) and reach dorsal roof to form dorsal lateral anastomotic vessel (DLAV) by 30 hpf. In contrast, the ISVs in miR-ntu1 morphants grew only halfway, less, or absent and usually failed to cross the horizontal myoseptum at 30 hpf, 48 hpf, even 60 hpf (Fig. 2d, e; Supplementary Fig. 2a–c). Furthermore, we found that the number of ECs in ISVs was significantly reduced in miR-ntu1-deficient embryos (Fig. 2f, g; Supplementary Fig. 2c). In addition, co-injection of miR-ntu1 duplex significantly alleviates the ISV branching angiogenic defects, suggesting the phenotype was specifically caused by miR-ntu1 downregulation (Supplementary Fig. 2a, b).

miR-ntu1 modulates the endothelial tip cell behaviors

As miR-ntu1 was involved in blood vessel formation during embryonic development, we supposed that it played a role in governing endothelial tip cell behaviors. To verify this hypothesis, we performed live imaging and time-lapse imaging analysis in *Tg(kdrl:EGFP)* embryos (Fig. 3a, b). It was revealed that filopodia extensions of ISV tip cells in miR-ntu1 morphants were shorter and less than those of controls (Fig. 3b, c). Furthermore, we examined the behavior of ISV tip cell nuclei using in vivo time-lapse imaging of *Tg(fli1a:nEGFP)* embryos (Fig. 3d). In the absence of miR-ntu1, the migration speed and proliferation of ISV tip cells was markedly reduced (Fig. 3d–f).

miR-ntu1 targets *dll4* and *mib1* in ECs

For identifying the targets of miR-ntu1, we did the target prediction using RNAhybrid [17]. In silico analysis, predicted miR-ntu1 potentially regulates hundreds of genes. A short list of target genes were selected for possible involvement in regulation of blood vessel phenotype of miR-ntu1 morphants, including *raf1, smo, lft1, ets1b, tbx20, ppm1k, fgf3, kdrb, dll4*, and *mib1*. In vitro luciferase assays demonstrated that miR-ntu1 duplex significantly inhibited the expression of luciferase-*dll4*-3′-UTR and luciferase-*mib1*-3′UTR compared with those of controls (Fig. 4a, b). To testify the functional interaction of miR-ntu1 and these two targets in vivo, we performed the fluorescence sensor assay in zebrafish embryo. It was confirmed that miR-ntu1 precursor repressed the expression of *mCherry-CAAX-dll4*-3′-UTR and *mCherry-mib1*-3′-UTR (Fig. 4c, d; Supplementary Fig. 3). Through whole-mount in situ hybridization analysis and Real-Time PCR, we found that mRNA levels of *dll4* and *mib1* in miR-ntu1 morphants were apparently increased (Fig. 5a, b). In addition, we found that the EGFP expression was elevated in *Tg(tp1:EGFP)* Notch reporter line (Fig. 5c), which expresses enhanced green fluorescent protein upon Notch activation. These results indicate that miR-ntu1 targets the 3′-UTR of *dll4* and *mib1* and thereby modulates Notch signaling pathway.

Reducing *dll4* and *mib1* restores the vascular defects in miR-ntu1-deficient embryos

Our results suggested that up-regulation of Notch signaling is the likely cause of angiogenic defects in miR-ntu1-deficient embryos. If this was the case, then inhibition of Notch signaling level would partially rescue the vascular phenotype of miR-ntu1-deficient embryos. To investigate this possibility, we knocked down *dll4* and *mib1* using morpholino oligos in miR-ntu1 morphants and then examined the vascular phenotypes including ISV length and EC numbers. Knockdown of *dll4* and *mib1* greatly normalized both sprout length and ISV cell numbers (Fig. 5d–f). Likewise, inhibition of Notch signaling using DAPT (γ-secretase inhibitor) significantly alleviated the vascular defects of miR-ntu1-deficient embryos (Fig. 5d–f).

Discussion

In present study, we showed that a ribosomal DNA-hosted microRNA, miR-ntu1, was highly expressed in zebrafish embryonic endothelial cells. Inhibition of miR-ntu1 impairs the endothelial tip cell behaviors and disrupts the intersegmental vessel branching angiogenesis. Unfortunately, there are several repeats of miR-ntu1 in different chromosomes of zebrafish. Therefore, it is hard to get the homozygous mutant. In silico analysis indicated that miR-ntu1 potentially targets hundreds of genes. With sensor assays, *mib1* and *dll4* were identified to be the possible downstream genes of miR-ntu1. Then, we demonstrated that the levels of *mib1, dll4,* and Notch signaling were elevated in miR-ntu1 morphants. In addition, inhibition of Notch partially restored the angiogenic defects of miR-ntu1 morphants. These results suggest that miR-ntu1 regulates zebrafish angiogenesis by modulating Notch signaling, depicted in a working model (Fig. 6).

Currently, accumulating evidences indicate that Notch signaling is vital for vascular morphogenesis including arterial and venous differentiation and endothelial tip and stalk cell specification during sprouting angiogenesis [18–24]. Dll4-Notch signaling is generally considered as a negative regulator of branching angiogenesis [20]. Mib1 is involved in the processing of Delta, a key endogenous ligand for Notch [25]. It has also been implicated in regulation of angiogenesis [26, 27]. In addition, a few of miRNAs were reported to regulate blood vessel formation by targeting the components of Notch signaling including *dll4* [28, 29] and *mib1* [14]. Here we describe an endothelial-expressed novel miRNA, miR-ntu1, which plays a crucial role in zebrafish angiogenesis via regulation of *dll4* and *mib1*, being consistent to that one gene which is targeted by many different miRNAs [30, 31]. Since the angiogenic defects caused by deficient of miR-10 and miR-30 were involved in Notch singling as well, we compared these with angiogenic defects in miR-ntu1 morphants. It was found that all these phenotypes were greatly restored by inhibition of Notch signaling. However, the angiogenic phenotypes caused by loss of miR-ntu1 function were more severe than those in miR-10 and miR-30 morphants [14, 28, 32], which might be explained at least by two possible reasons. The first one is that the expression level of miR-ntu1 is conspicuously higher than those of miR-10s (including miR-10a, b, c) and miR-30s (including miR-30a, b, c, d, e.) (Fig. 1d). The second one is that miR-ntu1

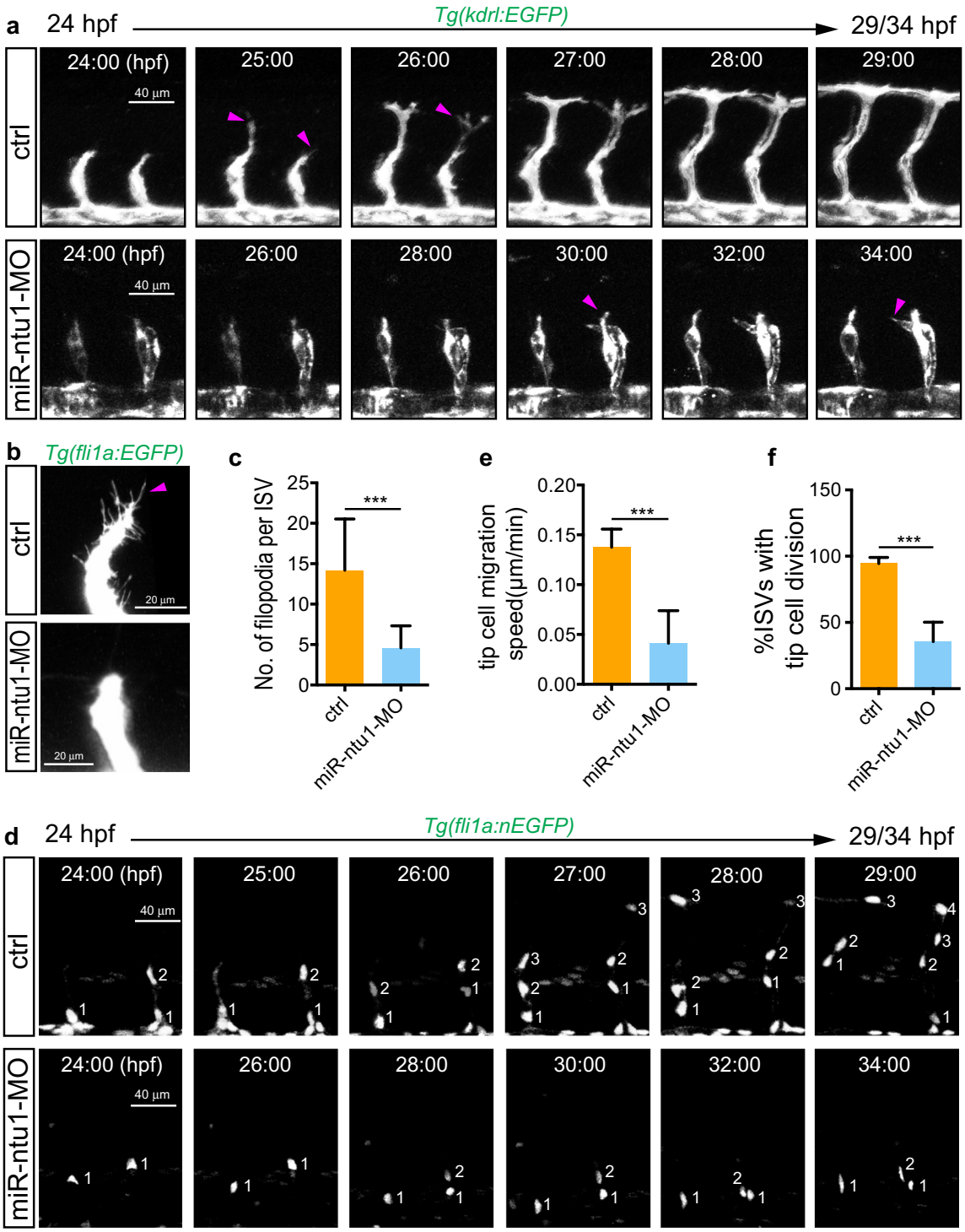

Fig. 3 miR-ntu1 regulates ISV tip cell behaviors. **a** Still images from in vivo time-lapse imaging analysis of ISV tip cell filopodia in *Tg(kdrl:EGFP)* embryos. Time (hpf) is noted at the top. Red arrowheads indicate filopodia extensions. **b** Confocal imaging analysis of ISV tip cell filopodia in *Tg(flila:EGFP)* embryos with HD detection setting. Red arrowhead indicates filopodia extensions. **c** ISV tip cell filopodia number in per ISV of control embryos and miR-ntu1 morphants (experiments repeated 2 times; control, $n=5$; miR-ntu1-MO, $n=6$; for each embryo three ISVs were analyzed). Mann–Whitney U test; $***P<0.001$. Time (hpf) is noted at the top. Nuclei of ISVs are numbered. **e** Migration speed of ISV tip cells (experiments repeated 2 times; control, $n=6$; miR-ntu1-MO, $n=7$). *T* test; $***P<0.001$. **f** Percentage of ISVs with tip cell division in control embryos and miR-ntu1 morphants (experiments repeated 2 times; control, $n=6$; miR-ntu1-MO, $n=8$). *T* test; $***P<0.001$

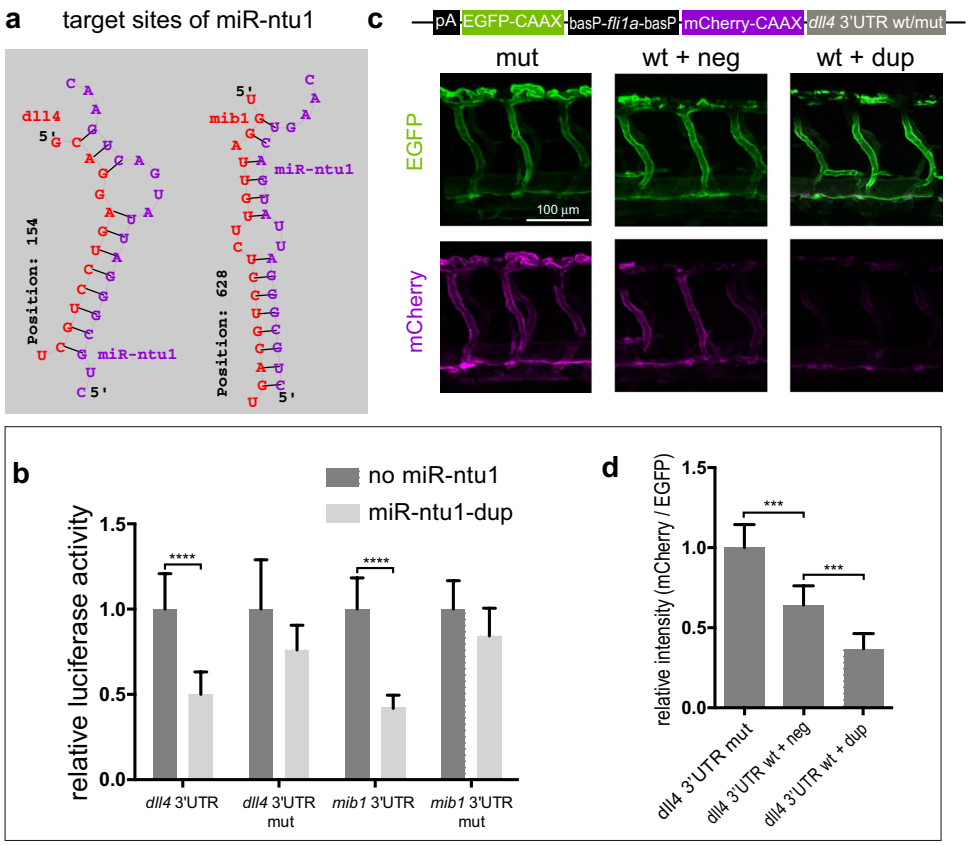

Fig. 4 miR-ntu1 targets *dll4* and *mib1*. **a** *dll4*-3′UTR and *mib1*-3′UTR target sites of miR-ntu1. **b** Overexpression of miR-ntu1 (miR-ntu1-pre) reduced *dll4*-3′UTR and *mib1*-3′UTR 1 luciferase activity in HeLa cells in vitro. Experiments were performed in triplicate (the experiments were repeated 3 times). *T* test; $^{****}P<0.0001$. **c** The confocal imaging analysis of EC autonomous miRNA sensors. The fluorescence expression was driven by *fli1a* enhancer, promoter element, and a basal promoter in opposite orientation. Each construct was microinjected into 1-cell stage zebrafish embryos with the Tol2 transposase mRNA. **d** Quantification of fluorescence in EC autonomous sensor assay. mCherry/EGFP ratio indicates comparison of relative voxel intensities. The experiments were repeated 2 times. For each embryo, 3 ISVs in the 7th, 8th, and 9th somites were used for quantification. Error bars represent standard deviation; for mutated 3′UTR control (mut), $n=4$; for wildtype 3′UTR + negative duplex control (wt + neg), $n=6$; for wildtype 3′UTR + miRNA duplex (wt + dup), $n=6$. One-way ANOVA; $^{***}P<0.001$

regulates two components of Notch signaling, both *dll4* and *mib1*, whereas miR-10 and miR-30 targets one of them.

To date, a few studies have reported the discovery and functions of rRNA-derived miRNAs or miRNA-like small RNAs [13, 33–36]. Many rRNA-annotated fragments of miRNA-like size have been detected in high-throughput RNA sequencing studies; however, the sequences mapped to ribosomal RNAs (rRNAs) were mostly considered to be degradation products, and therefore discarded [33]. In present study, we identified a ribosomal DNA-hosted small RNA in a deep sequencing analysis of zebrafish ECs. This small RNA was predicted as a miRNA by miRDeep2 algorithm. In addition, the frequency curve of miR-ntu1 mature sequence mapped to the rDNA displayed a high peak (Fig. 1b), with a single sequence having 21,242 read counts, suggesting the mature sequence was not generated by random degradation products of rRNA. Moreover, miR-ntu1 was validated by northern blot and custom-designed Taqman PCR analysis. Furthermore, it was revealed to play a crucial role in zebrafish blood vessel formation. Taken together, our findings provide a notable case that a miRNA hosted in ribosomal DNA is involved in vertebrate development.

Materials and methods

Ethics statement

All animal experimentation was carried out in accordance with the NIH Guidelines for the care and use of laboratory animals (http://oacu.od.nih.gov/regs/index.htm) and ethically approved by the Administration Committee of Experimental Animals, Jiangsu Province, China (Approval ID: SYXK (SU)2007–0021).

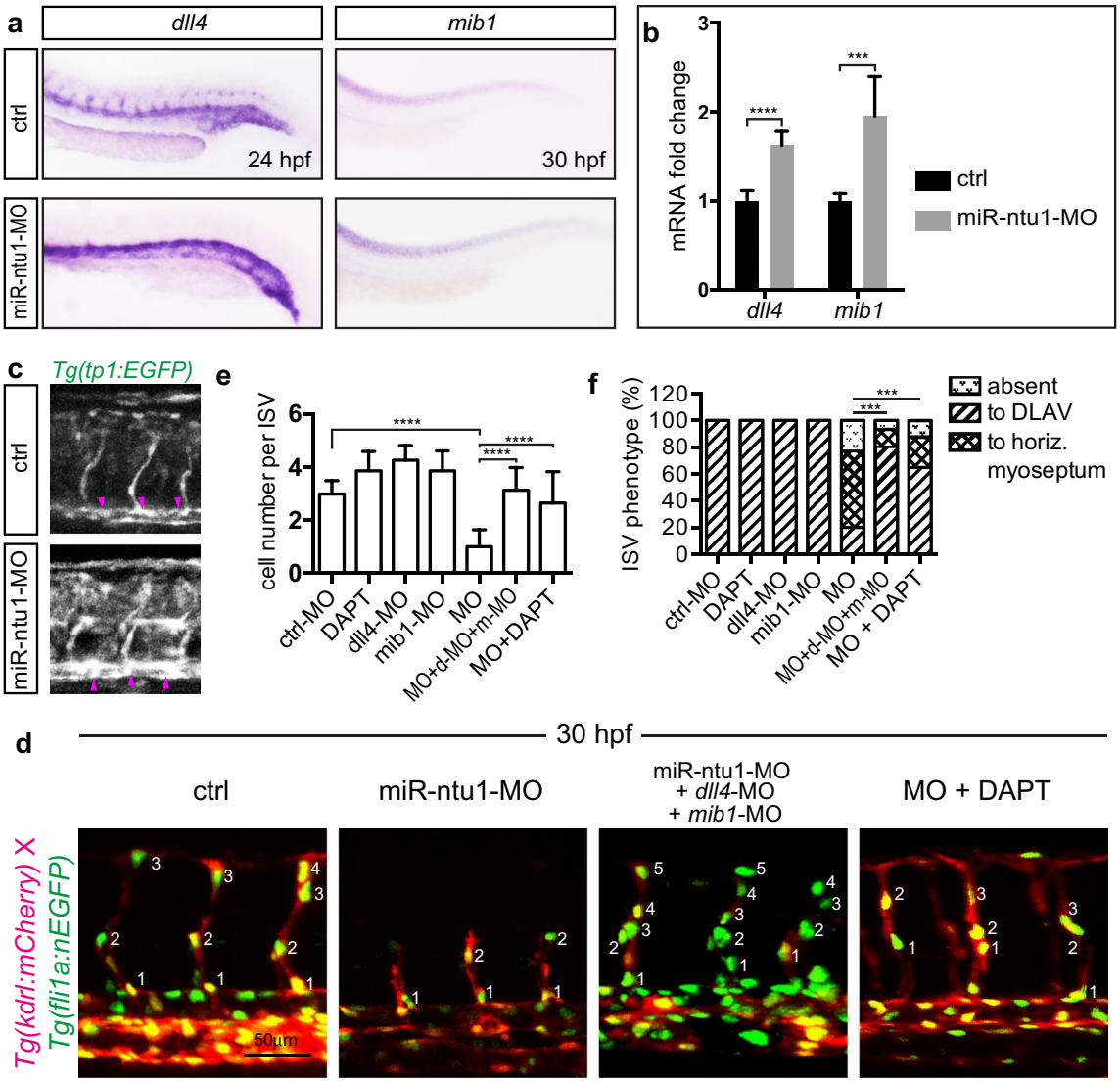

Fig. 5 Reducing Notch signaling rescued the vascular defects in miR-ntu1-deficient embryos. **a** Whole-mount in situ hybridization analysis of *dll4* and *mib1* expression in control zebrafish embryos and miR-ntu1 morphants. **b** Relative mRNA levels of zebrafish *dll4* and *mib1* in 24 hpf control or miR-ntu1 morphants. (the experiments were repeated 2 times; independent samples = 6). *T* test; ***$P < 0.0001$. **c** The confocal imaging analysis of control and miR-ntu1-MO-injected *Tg(tp1:EGFP)* embryos, showing Notch signaling was up-regulated in miR-ntu1 morphants. Arrowheads indicate dorsal aorta. **d** Confocal images of trunk vessels at 30 hpf in *Tg(kdrl:mCherry)* × *Tg(fli1a:nEGFP)* embryos. **e** Statistical analysis of ECs nuclei number in ISV (d-MO, *dll4*-MO; m-MO, *mib1*-MO), experiments repeated 3 times. (control, $n = 17$; DAPT, $n = 17$; *dll4*-MO, $n = 17$; *mib1*-MO, $n = 17$; miR-ntu1-MO, $n = 17$; miR-ntu1-MO + *dll4*-MO + *mib1*-MO, $n = 33$; miR-ntu1-MO + DAPT, $n = 17$). One-way ANOVA; ****$P < 0.0001$. **f** Quantification of embryos with indicated ISV phenotypes of different sprout lengths. (control, $n = 17$; DAPT, $n = 17$; *dll4*-MO, $n = 17$; *mib1*-MO, $n = 17$; miR-ntu1-MO, $n = 17$; miR-ntu1-MO + *dll4*-MO + *mib1*-MO, $n = 33$; miR-ntu1-MO + DAPT, $n = 17$), experiments repeated 3 times. For each embryo, 5 ISVs in the 6th, 7th, 8th, 9th and 10th somites were analyzed. χ^2; ***$P < 0.001$

Zebrafish

The study was conducted conforming to the local institutional laws and the Chinese law for the Protection of Animals. Zebrafish embryos and adult were raised and maintained under standard conditions as we previously described [37, 38]. Transgenic zebrafish lines,

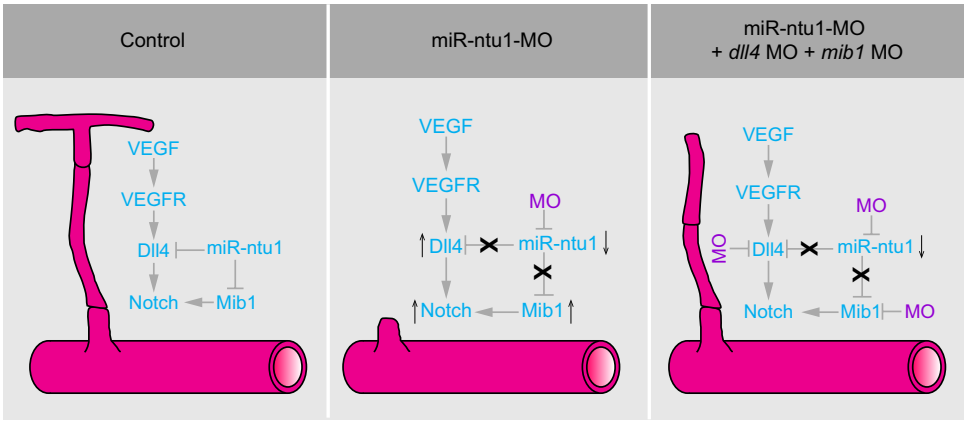

Fig. 6 A working model for the function of miR-ntu1 in angiogenesis. Loss of miR-ntu1 leads to up-regulation of the Notch signaling pathways, which inhibits angiogenesis. Reducing *dll4* and *mib1* in miR-ntu1 morphants alleviated the angiogenetic defects

Tg(fli1:nEGFP), *Tg(kdrl:EGFP)*, and *Tg(kdrl:mCherry)*, were used as described in previous work [14, 28, 39].

Injection of morpholinos, microRNA precursor, and construct

Morpholino antisense oligomers (MO, Gene Tools) were prepared according to the manufacturer's protocol. The MO and miRNA precursor sequences used are listed in the following:

Dre-miR-ntu1-MO (5 ng), 5′-GAGGCGTTCAGTCATAATCCCGCAG-3′;
Mib1-MO (6 ng), 5′-GCAGCCTCACCTGTAGGCGCACTGT-3′;
Dll4-MO (3 ng), 5′-GTTCGAGCTTACCGGCCACCCAAAG-3′;
Control-MO (8 ng), 5′-CCTCTTACCTCAGTTACAATTTATA-3′;

0.025 pmol miR-ntu1 and a universal scrambled negative control were injected into embryos at 1-2-cell stage.

Tg(fli1a:mCherry-CAAX-dll4 3′UTR::fli1a:EGFP-CAAX) and *Tg(fli1a:mCherry-mib1 3′UTR::fli1a:EGFP)* construct and Tol2 transposase mRNA mixture were injected into 1-2-cell stage wildtype fertilized egg (1 ng / embryo).

Gene and microRNA expression analysis by quantitative PCR, RT-PCR, and northern blot

Total RNA of zebrafish embryos was isolated with Trizol (Invitrogen). Quantity of extracted RNA was analyzed using Nanodrop according to the manufacturer's instructions, followed by cDNA synthesis using the Transcriptor First Strand cDNA Synthesis Kit (Roche) according to the manufacturer's instructions. Synthesized cDNA was stored at − 20 °C. The custom-designed dre-miR-ntu1 TaqMan® MicroRNA Assays were purchased from Thermo Fisher Scientific Inc. The experiments were performed according to the manufacturer's instructions. For quantitative PCR, experiments were repeated 3 times, 5–10 embryos per pool, 2 pools per treatment, 3 technical replicates per run. The primers for RT-PCR and real-time PCR are listed, for *ef1a* (Accession: NM_131263.1):

Forward primer, 5′-TGATCTACAAATGCGGTGGA-3′;
Reverse primer, 5′-CAATGGTGATACCACGCTCA-3′.
For *dll4* (Accession: NM_001079835.1):
Forward primer, 5′-attccccatgctttcacaag-3′;
Reverse primer, 5′-tccatccttctctcgcagtt-3′.
For *mib1* (NM_173286.3)
Forward primer, 5′-gaactgtgcaagcctgatga-3′;
Reverse primer, 5′-cagtggcatcctccatacct-3′.

Total RNA was extracted from control and miR-ntu1-MO-injected zebrafish embryos at 30 hpf using Trizol (Invitrogen). Northern blotting for miR-ntu1 was performed as described previously [28]. Briefly, 15 μg of zebrafish Total RNA was loaded onto an 12% acrylamide gel with 8 mol/L urea, electro-transferred to Nylon membrane (GE Healthcare), and hybridized with ^{32}P-end-labeled species-specific LNA probes at 50 °C for 16 h. Membranes were washed twice for 10 min each time.

Whole-mount in situ hybridization

Whole-mount in situ hybridization with antisense RNA probes (*dll4, mib1*) was performed as previously described [14, 28].

Luciferase assays and microRNA sensor assay in zebrafish

The dual-luciferase reporter constructs were all derived from the psiCHECK-2 vector (Promega). Zebrafish *mib1* 3′UTR/mutated *mib1* 3′UTR and *dll4* 3′UTR/mutated *dll4* 3′UTR

were inserted between the XhoI–NotI restriction sites in the multiple cloning regions in the 3′ UTR of the hRluc gene. Advantage® 2 DNA Polymerase Mix (Clontech Laboratories, Inc.) is used for the PCR amplification. psiCheck2-*mib1*/*dll4*-3′UTR reporter assay construct was transfected into HeLa cells with or without miR-ntu1 duplex. Reporter assays were performed with the Dual-Luciferase Reporter Assay System (Promega). 24 h after transfection, cells were lysed and Luciferase activity measured as indicated by the manufacturer. Reporter activity was adjusted for the internal Renilla luciferase controls and is expressed as relative to control.

The following two pairs of primers were used for cloning the insertion fragment.

Mib1-3′UTR-Xho1-left: 5′-ATCCGCTCGAGTCTCATAAGCACCTTCCCCG-3′
Mib1-3′UTR-Not1-right: 5′-ATAGCGGCCGCTCTCAGACCAGGGCAGTTTT-3′
Dll4-3′UTR- Xho1-left: 5′-ATCCGCTCGAGCAAGGGACTCCGTGTACCAGT-3′
Dll4-3′UTR- Not1-right: 5′-ATAGCGGCCGCCTGGGCACAAACATAGCACTC-3′.

The plasmids with mutated target sequences of *dll4* and *mib1* 3′UTR were derived from these above plasmids. The constructs for microRNA sensor assay in zebrafish were synthesized and sub-cloned by Union-Biotech (Shanghai). The same sequences of *dll4* and *mib1* mRNA 3′UTR in luciferase reporter constructs were included in the microRNA sensor assay transgenic constructs. The procedure of microinjection of these microRNA sensor assay plasmids was as previously described [40]. The florescence-labeled transgenic zebrafish lines for sensor assay were photographed using confocal microscope (details in "Imaging" section). mCherry/EGFP ratio indicates relative voxel intensities derived from 3-dimensional reconstructions of confocal images. EGFP was used as a control.

Drug treatment

DAPT, a γ-secretase inhibitor, was purchased from Sigma-Aldrich and dissolved in DMSO. DAPT was used at a final concentration of 100 μM diluted as our pervious description [14]. Egg water containing DMSO alone was utilized as control.

MicroRNA library preparation and sequencing, novel miRNA prediction, and target prediction

Total RNA was isolated using Trizol reagent (Thermo Scientific) according to the manufacturer's protocol. Quality of total RNA was controlled using Nanodrop (Thermo Scientific) and 21,000 Bioanalyzer (Agilent Technologies) analyses. Illumina sequencing libraries were prepared according to the Illumina preparation kit protocol. MicroRNA libraries generated from zebrafish ECs were sequenced on the Genome Analyzer 2 (Illumina). RNA sequences detected by small RNA deep sequencing were mapped to the genome and analyzed using MirDeep2. Target prediction of miR-ntu1 was carried out by RNAhybrid (http://bibiserv.techfak.uni-bielefeld.de/rnahybrid/).

Imaging

For confocal imaging of blood vessel development in *Tg(kdrl:EGFP)* and *Tg(fli1a:nEGFP)* zebrafish embryos, they were anesthetized with egg water/0.16 mg/mL tricaine/1% 1-phenyl-2-thiourea (Sigma) and embedded in 0.6% low melting agarose. Confocal imaging was performed with a Leica TCS-SP5 LSM. Analysis was performed using Imaris software. For the results of in situ hybridization, images were recorded under Olympus stereomicroscope MVX10 and a DP70 camera.

Statistics

Statistical analysis was performed using GraphPad Prism® software. *T* test, Mann–Whitney U test, one-way ANOVA, and Chi-square were used. ($P < 0.05$).

Acknowledgements This work was supported by the National Natural Science Foundation of China 81570447, 81870359; Natural Science Foundation from Jiangsu Province 17KJA180008, SWYY-048, and BK20180048.

References

1. Bartel DP (2004) MicroRNAs: genomics, biogenesis, mechanism, and function. Cell 116(2):281–297
2. Ambros V (2004) The functions of animal microRNAs. Nature 431(7006):350–355. https://doi.org/10.1038/nature02871
3. Bartel DP (2009) MicroRNAs: target recognition and regulatory functions. Cell 136(2):215–233. https://doi.org/10.1016/j.cell.2009.01.002
4. He S, Su H, Liu C, Skogerbo G, He H, He D, Zhu X, Liu T, Zhao Y, Chen R (2008) MicroRNA-encoding long non-coding RNAs. BMC Genom 9:236. https://doi.org/10.1186/1471-2164-9-236
5. Saraiya AA, Wang CC (2008) snoRNA, a novel precursor of microRNA in *Giardia lamblia*. PLoS Pathog 4(11):e1000224. https://doi.org/10.1371/journal.ppat.1000224
6. Kloosterman WP, Plasterk RH (2006) The diverse functions of microRNAs in animal development and disease. Dev Cell 11(4):441–450. https://doi.org/10.1016/j.devcel.2006.09.009
7. Stefani G, Slack FJ (2008) Small non-coding RNAs in animal development. Nat Rev Mol Cell Biol 9(3):219–230. https://doi.org/10.1038/nrm2347
8. Hata A (2013) Functions of microRNAs in cardiovascular biology and disease. Annu Rev Physiol 75:69–93. https://doi.org/10.1146/annurev-physiol-030212-183737

9. Condorelli G, Latronico MV, Cavarretta E (2014) microRNAs in cardiovascular diseases: current knowledge and the road ahead. J Am Coll Cardiol 63(21):2177–2187. https://doi.org/10.1016/j.jacc.2014.01.050
10. Liu D, Krueger J, Le Noble F (2011) The role of blood flow and microRNAs in blood vessel development. Int J Dev Biol 55(4–5):419–429. https://doi.org/10.1387/ijdb.103220dl
11. Small EM, Olson EN (2011) Pervasive roles of microRNAs in cardiovascular biology. Nature 469(7330):336–342. https://doi.org/10.1038/nature09783
12. Zentner GE, Saiakhova A, Manaenkov P, Adams MD, Scacheri PC (2011) Integrative genomic analysis of human ribosomal DNA. Nucleic Acids Res 39(12):4949–4960. https://doi.org/10.1093/nar/gkq1326
13. Chak LL, Mohammed J, Lai EC, Tucker-Kellogg G, Okamura K (2015) A deeply conserved, noncanonical miRNA hosted by ribosomal DNA. RNA 21(3):375–384. https://doi.org/10.1261/rna.049098.114
14. Wang X, Ling CC, Li L, Qin Y, Qi J, Liu X, You B, Shi Y, Zhang J, Jiang Q, Xu H, Sun C, You Y, Chai R, Liu D (2016) MicroRNA-10a/10b represses a novel target gene mib1 to regulate angiogenesis. Cardiovasc Res 110(1):140–150. https://doi.org/10.1093/cvr/cvw023
15. Friedlander MR, Chen W, Adamidi C, Maaskola J, Einspanier R, Knespel S, Rajewsky N (2008) Discovering microRNAs from deep sequencing data using miRDeep. Nat Biotechnol 26(4):407–415. https://doi.org/10.1038/nbt1394
16. Friedlander MR, Mackowiak SD, Li N, Chen W, Rajewsky N (2012) miRDeep2 accurately identifies known and hundreds of novel microRNA genes in seven animal clades. Nucleic Acids Res 40(1):37–52. https://doi.org/10.1093/nar/gkr688
17. Rehmsmeier M, Steffen P, Hochsmann M, Giegerich R (2004) Fast and effective prediction of microRNA/target duplexes. RNA 10(10):1507–1517. https://doi.org/10.1261/rna.5248604
18. Phng LK, Gerhardt H (2009) Angiogenesis: a team effort coordinated by notch. Dev Cell 16(2):196–208. https://doi.org/10.1016/j.devcel.2009.01.015
19. Hellstrom M, Phng LK, Hofmann JJ, Wallgard E, Coultas L, Lindblom P, Alva J, Nilsson AK, Karlsson L, Gaiano N, Yoon K, Rossant J, Iruela-Arispe ML, Kalen M, Gerhardt H, Betsholtz C (2007) Dll4 signalling through Notch1 regulates formation of tip cells during angiogenesis. Nature 445(7129):776–780. https://doi.org/10.1038/nature05571
20. Leslie JD, Ariza-McNaughton L, Bermange AL, McAdow R, Johnson SL, Lewis J (2007) Endothelial signalling by the Notch ligand Delta-like 4 restricts angiogenesis. Development 134(5):839–844. https://doi.org/10.1242/dev.003244
21. Siekmann AF, Lawson ND (2007) Notch signalling limits angiogenic cell behaviour in developing zebrafish arteries. Nature 445(7129):781–784. https://doi.org/10.1038/nature05577
22. Lobov IB, Renard RA, Papadopoulos N, Gale NW, Thurston G, Yancopoulos GD, Wiegand SJ (2007) Delta-like ligand 4 (Dll4) is induced by VEGF as a negative regulator of angiogenic sprouting. Proc Natl Acad Sci USA 104(9):3219–3224. https://doi.org/10.1073/pnas.0611206104
23. Hasan SS, Tsaryk R, Lange M, Wisniewski L, Moore JC, Lawson ND, Wojciechowska K, Schnittler H, Siekmann AF (2017) Endothelial Notch signalling limits angiogenesis via control of artery formation. Nat Cell Biol 19(8):928–940. https://doi.org/10.1038/ncb3574
24. Pitulescu ME, Schmidt I, Giaimo BD, Antoine T, Berkenfeld F, Ferrante F, Park H, Ehling M, Biljes D, Rocha SF, Langen UH, Stehling M, Nagasawa T, Ferrara N, Borggrefe T, Adams RH (2017) Dll4 and Notch signalling couples sprouting angiogenesis and artery formation. Nat Cell Biol 19(8):915–927. https://doi.org/10.1038/ncb3555
25. Itoh M, Kim CH, Palardy G, Oda T, Jiang YJ, Maust D, Yeo SY, Lorick K, Wright GJ, Ariza-McNaughton L, Weissman AM, Lewis J, Chandrasekharappa SC, Chitnis AB (2003) Mind bomb is a ubiquitin ligase that is essential for efficient activation of Notch signaling by Delta. Dev Cell 4(1):67–82
26. Lawson ND, Scheer N, Pham VN, Kim CH, Chitnis AB, Campos-Ortega JA, Weinstein BM (2001) Notch signaling is required for arterial-venous differentiation during embryonic vascular development. Development 128(19):3675–3683
27. Jensen LD, Cao Z, Nakamura M, Yang Y, Brautigam L, Andersson P, Zhang Y, Wahlberg E, Lanne T, Hosaka K, Cao Y (2012) Opposing effects of circadian clock genes bmal1 and period2 in regulation of VEGF-dependent angiogenesis in developing zebrafish. Cell Rep 2(2):231–241. https://doi.org/10.1016/j.celrep.2012.07.005
28. Jiang Q, Lagos-Quintana M, Liu D, Shi Y, Helker C, Herzog W, le Noble F (2013) miR-30a regulates endothelial tip cell formation and arteriolar branching. Hypertension 62(3):592–598. https://doi.org/10.1161/HYPERTENSIONAHA.113.01767
29. Bridge G, Monteiro R, Henderson S, Emuss V, Lagos D, Georgopoulou D, Patient R, Boshoff C (2012) The microRNA-30 family targets DLL4 to modulate endothelial cell behavior during angiogenesis. Blood 120(25):5063–5072. https://doi.org/10.1182/blood-2012-04-423004
30. Krek A, Grun D, Poy MN, Wolf R, Rosenberg L, Epstein EJ, MacMenamin P, da Piedade I, Gunsalus KC, Stoffel M, Rajewsky N (2005) Combinatorial microRNA target predictions. Nat Genet 37(5):495–500. https://doi.org/10.1038/ng1536
31. Hon LS, Zhang Z (2007) The roles of binding site arrangement and combinatorial targeting in microRNA repression of gene expression. Genome Biol 8(8):R166. https://doi.org/10.1186/gb-2007-8-8-r166
32. Hassel D, Cheng P, White MP, Ivey KN, Kroll J, Augustin HG, Katus HA, Stainier DY, Srivastava D (2012) MicroRNA-10 regulates the angiogenic behavior of zebrafish and human endothelial cells by promoting vascular endothelial growth factor signaling. Circ Res 111(11):1421–1433. https://doi.org/10.1161/CIRCRESAHA.112.279711
33. Wei H, Zhou B, Zhang F, Tu Y, Hu Y, Zhang B, Zhai Q (2013) Profiling and identification of small rDNA-derived RNAs and their potential biological functions. PLoS ONE 8(2):e56842. https://doi.org/10.1371/journal.pone.0056842
34. Yoshikawa M, Fujii YR (2016) Human ribosomal RNA-derived resident microRNAs as the transmitter of information upon the cytoplasmic cancer stress. Biomed Res Int 2016:7562085. https://doi.org/10.1155/2016/7562085
35. Son DJ, Kumar S, Takabe W, Kim CW, Ni CW, Alberts-Grill N, Jang IH, Kim S, Kim W, Won Kang S, Baker AH, Woong Seo J, Ferrara KW, Jo H (2013) The atypical mechanosensitive microRNA-712 derived from pre-ribosomal RNA induces endothelial inflammation and atherosclerosis. Nat Commun 4:3000. https://doi.org/10.1038/ncomms4000
36. Li Y, Zeng A, Han XS, Li G, Li YQ, Shen B, Jing Q (2017) Small RNAome sequencing delineates the small RNA landscape of pluripotent adult stem cells in the planarian *Schmidtea mediterranea*. Genom Data 14:114–125. https://doi.org/10.1016/j.gdata.2017.10.004
37. Huang Y, Wang X, Wang X, Xu M, Liu M, Liu D (2013) Nonmuscle myosin II-B (myh10) expression analysis during zebrafish embryonic development. Gene Expr Patterns 13(7):265–270. https://doi.org/10.1016/j.gep.2013.04.005
38. Xu M, Liu D, Dong Z, Wang X, Wang X, Liu Y, Baas PW, Liu M (2014) Kinesin-12 influences axonal growth during zebrafish neural development. Cytoskeleton 71(10):555–563. https://doi.org/10.1002/cm.21193

39. Krueger J, Liu D, Scholz K, Zimmer A, Shi Y, Klein C, Siekmann A, Schulte-Merker S, Cudmore M, Ahmed A, le Noble F (2011) Flt1 acts as a negative regulator of tip cell formation and branching morphogenesis in the zebrafish embryo. Development 138(10):2111–2120. https://doi.org/10.1242/dev.063933
40. Lv F, Zhu C, Yan X, Wang X, Liu D (2017) Generation of a mef2aa:EGFP transgenic zebrafish line that expresses EGFP in muscle cells. Fish Physiol Biochem 43(1):287–294. https://doi.org/10.1007/s10695-016-0286-3